Geomechanics and Engineering, *Vol. 21, No. 1 (2020) 63-71*
DOI: https://doi.org/10.12989/gae.2020.21.1.063

Strength degradation of a natural thin-bedded rock mass subjected to water immersion and its impact on tunnel stability

Yuting Zhang*, Xiuli Ding, Shuling Huang, Yongjin Wu and Jun He

Key Laboratory of Geotechnical Mechanics and Engineering of the Ministry of Water Resources, Changjiang River Scientific Research Institute, Wuhan, Hubei, China

(Received January 17, 2020, Revised March 7, 2020, Accepted March 10, 2020)

Abstract. Strength anisotropy is a typical feature of thin-bedded rock masses and their strength will be degraded subjected to water immersion effect. Such effect is crucial for the operation of hydropower plant because the impoundment lifts the water level of upstream reservoir and causes the rock mass of nearby slopes saturated. So far, researches regarding mechanical property of natural thin-bedded rock masses and their strength variation under water immersion based on field test method are rarely reported. This paper focuses on a thin-bedded stratified rock mass and carries out field test to investigate the mechanical property and strength variation characteristics. The field test is highlighted by samples which have a large shear dimension of 0.5 m*0.5 m, representing a more realistic in-situ situation than small size specimen. The test results confirm the anisotropic nature of the concerned rock mass, whose shear strength of host rocks is significantly larger than that of bedding planes. Further, the comparison of shear strength parameters of the thin-bedded rock mass under natural and saturated conditions show that for both host rocks and bedding planes, the decreasing extent of cohesion values are larger than friction values. The quantitative results are then adopted to analyze the influence of reservoir impoundment of a hydropower plant on the surrounding rock mass stability of diversion tunnels which are located in the nearby slope bank. It is evaluated that after reservoir impoundment, the strength degradation induced incremental deformations of surrounding rock mass of diversion tunnels are small and the stresses in lining structure are acceptable. It is therefore concluded that the influences of impoundment are small and the stability of diversion tunnels can be still achieved. The finings regarding field test method and its results, as well as the numerical evaluation conclusions are hoped to provide references for rock projects with similar concerns.

Keywords: thin-bedded rock mass; water immersion; field test; strength anisotropy; mechanical property degradation

1. Introduction

Bedding planes and schistosities make stratified rock mass highly anisotropic and govern its deformation and failure pattern. A rational estimate of mechanical properties considering the inherent anisotropic feature is crucial for the stability evaluation of tunnels and slopes excavated in stratified rock masses. A thin-bedded stratified rock mass has poor intactness, thin layer structure with one prevailing orientation. The thickness of host rocks is typically smaller than 10cm. For weak bedding planes or schistosities, they cannot withstand drilling disturbance and the cores are always broken along the stratification planes. Therefore, conventional core drilling sampling technique and corresponding laboratory testing procedures are effective for stratified rock masses with medium to thick bedded structure, but not suitable for those with thin layers. Hoek *et al.* (Hoek *et al.* 2005) categorized such stratified rock mass as laminated or sheared structure in the GSI system and suggested an empirical approach to determine its mechanical parameters. Rehman *et al.* (Rehman *et al.* 2019) extended the Q index originally used for tunnel support in moderately jointed and massive rocks to highly stressed jointed rock mass based on an empirical approach. In addition, a number of scholars (Gokceoglu and Aksoy 2010, Fortsakis *et al.* 2012, Aydan *et al.* 2013, Marinos 2019) have made meaningful extensions to these empirical approaches and greatly improved the adaptability of classification systems for stratified rock masses. Another notable approach to estimate mechanical parameters is based on known parameters and using advanced algorithms, such as neutral network and ANFIS technique, to predict the mechanical parameters (Alemdag *et al.* 2015, Umrao *et al.* 2018). Besides these indirect methods, some scholars (Palmström and Singh 2001, Ishida *et al.* 2010) have conducted in-situ tests on rock masses and compared the results with indirect estimating method and demonstrated the significance of field tests.

Water content is another important factor affecting the mechanical properties of rock masses. On one hand, high porous and hydrophilic rocks can absorb moisture easily so water and rock minerals can take physical and chemical effect, leading to mechanical degradation. Many scholars (Zhao *et al.* 2016, Kim and Changani 2016, Roy *et al.* 2017, Gu *et al.* 2018, Kundu *et al.* 2018, Tang *et al.* 2018, Zhang *et al.* 2018, Zhou *et al.* 2018, Xing *et al.* 2019) studied this issue and obtained results that are helpful for characterizing the mechanical property variation of rock specimen subjected to water immersion effect. It is generally found

*Corresponding author, Ph.D., Associate Professor
E-mail: magicdonkey@163.com

ISSN: 2005-307X (Print), 2092-6219 (Online)

that the mechanical parameters under fully saturated state decrease significantly compared to the parameters under natural state. On the other hand, for rock masses containing hydrophilic infillings, their mechanical properties will be degraded subjected to water infiltration. Several researchers (Pellet *et al.* 2013, Liu and Sheng 2019, Zhao *et al.* 2017, Liu *et al.*, 2019) studied the influences of water content variation on rock specimen containing joints or fractures and concluded that the discontinuities play a dominant role.

In general, the above literature review indicates that the primary method for determining mechanical parameters of highly anisotropic stratified rock masses follows an empirical and indirect way, while field tests using specimen in large size are rarely reported. Moreover, investigations on the degradation of discontinuities due to water effect are always carried out using small size specimen containing limited number of rock joints, rather than field tests directly performing on stratified rock masses of thin layer structure. Although the non-experimental approaches are established based on experiences and sophisticated tools, it is intuitively better to obtain the mechanical properties based on experiments, because large size specimen containing many bedding planes are difficult to obtain using core drilling method. Further, laboratory experiments may achieve excellent laws for rock specimen exposed to water, but cannot provide a rational estimate of mechanical parameters of highly anisotropic rock masses at a larger scale due to the lack of representativeness of small size specimen. Therefore, these results, due to the inherent methodological insufficiency, are difficult to associate with practical engineering problems where the concerned anisotropic stratified rock masses cover a wide range and will be subjected to a remarkable effect of water immersion.

In the present case study, a stratified rock mass containing very thin-bedded rock layers is attached with great importance because its bearing capacity and property variation is crucial for the focused project, which is an ongoing large scale hydropower plant in China. In order to address the primary engineering concerns, field tests were performed in-situ to investigate the mechanical characteristics and strength variation laws for thin-bedded rock masses under both natural and water-saturated conditions. The rock mass samples were all prepared in field and the shear dimension is 0.5 m*0.5 m. The obtained field test results are further used in a numerical analysis aiming to evaluate rock mass stability subjected to the impoundment of upstream reservoir.

2. An outline of the concerned issue where the stratified rock mass plays an important role

After nearly two decades of high-speed development of hydropower resources, China in the future will have more and more large scale hydropower plants completed. Reservoir impoundment is a necessary procedure of power generation. It lifts the water level of upstream and leads to changes in the hydrogeological conditions of rock masses in the nearby slope banks. As a result, the slope rock mass within the water rising range are fully saturated, causing potential threats to the stability of nearby tunnels, such as

Fig. 1 Upstream view of Wudongde dam site in year 2016

diversion tunnels and headrace tunnels which are always excavated in the slope banks. Because the increase in the water content of surrounding rock mass of tunnels will degrade the mechanical properties, resulting in decreased bearing capacity.

To look into this issue, the ongoing Wudongde hydropower plant in southwest China is focused. It is located on the Jinshajiang River and is China's third largest as well as world's seventh largest hydropower plant. Five diversion tunnels are planned for water conveyance purpose during dam construction period. Nos. 3, 4, and 5 diversion tunnels are placed on the right bank and adverse geological conditions are identified on their upstream sections. The strata of the adverse geological conditions are mainly thin- and ultra-thin-layered marbleized dolomite and is characterized by its high anisotropy. Although the diversion tunnels were successfully excavated with required stability (Ding *et al.* 2017) and are currently put into use (Figure 1), future impoundment will lift the water level of upstream reservoir and place the surrounding rock mass of diversion tunnels near the slope in a potentially hazardous stability condition.

As this kind of thin-bedded rock masses are easily damaged by core drilling method and also inevitably disturbed by sample package and transportation procedures, it is difficult to obtain reasonable laboratory results using samples whose representativeness of the field situation is clearly far from sufficient. Base on this understanding, field tests were performed to investigate the mechanical characteristics and variation laws of thin-bedded rock masses under natural and water-saturated conditions.

3. Field tests using large size rock mass specimen

3.1 Test preparation

The distribution of strata conditions is firstly examined. An area having the same lithology and rock mass structure condition with the adverse geological condition of diversion tunnels is chosen as the field test location. A test pit with a dimension of 8 m×2 m×2 m (length×width×depth) is excavated (Fig. 2). To facilitate the preparation of rock mass samples, the test pit is excavated in such a way that its length direction is perpendicular to the strike of bedding planes of the thin-bedded rock mass and its width direction

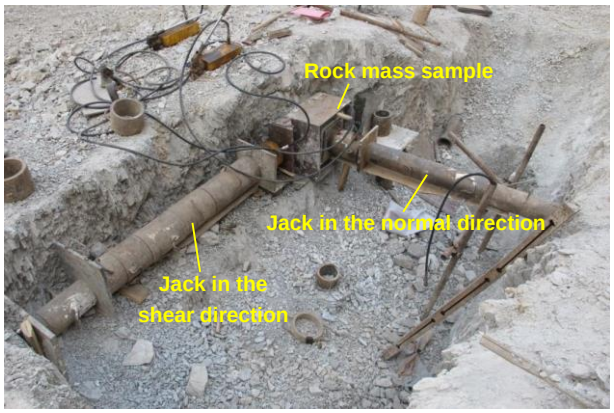

Fig. 2 Layout of rock mass sample and test equipment in the test pit

Fig. 3 Rock mass samples soaked in water for 48h

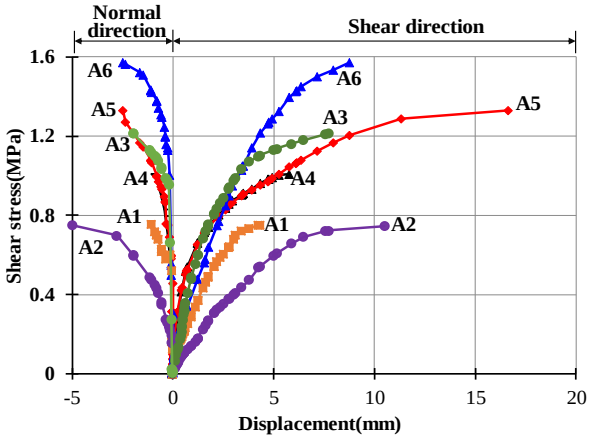

(a) Natural state

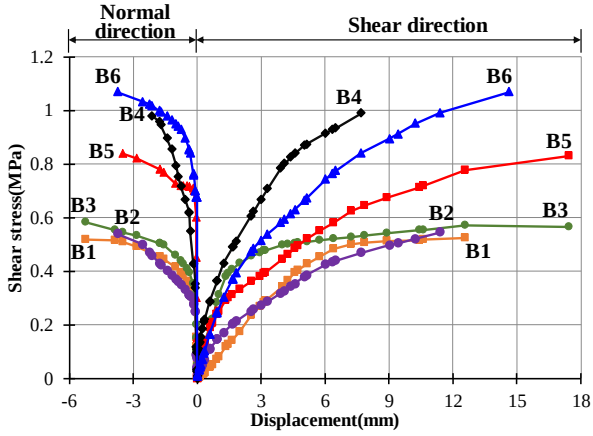

(b) Saturated state

Fig. 4 Shear stress *versus* displacement curves with shear loading direction perpendicular to bedding plane strike

is parallel to the strike of bedding planes. All rock mass samples are prepared at the walls of the test pit. The shear dimension of each sample is about 0.5 m×0.5 m. Each sample is firstly enfolded with a steel mold and then the normal and shear loads are applied horizontally to the mold.

Based on laboratory test results, the natural water content for rocks of similar lithology with the field test is 0.21%, and the saturated water content is 0.37%. It should be noted that the rock samples used in water content test are different in size with field rock mass samples, but the obtained data still provide useful information regarding the description of the natural and saturated states for rocks with the concerned strata conditions.

Moreover, it is believed that the results obtained in the studied diversion tunnel would be more valuable by putting the field test site in the diversion tunnel directly. However, the diversion tunnels, as displayed in Fig. 1, have been all put into use at the time of field test. If the field test cannot be conducted until reservoir impoundment, then any meaningful and practical advice will be in vain. It is due to this fact that the field test was conducted at a place of similar lithological condition with the site of diversion tunnel.

3.2 Test schemes

Two groups of direct shear tests are planned. The first group aims to obtain the shear strength perpendicular to the strikes of bedding planes so its shear loading direction is perpendicular to the strike and normal load is applied with a fixed level parallel to the strike. The second group aims obtain the shear strength parallel to the strikes of bedding planes so its shear loading direction and normal load are both determined accordingly.

When performing the direct shear tests, the normal load is firstly applied and maintains at certain level. Shear load is then applied from zero and increases slowly. The rock mass sample undertakes an increasing shear load until shear failure finally takes place. The peak value of applied shear load is recorded. By dividing the shear area, the shear strength of rock mass sample can be calculated.

The above two groups of direct shear tests are firstly performed using rock mass samples under natural state. Based on the recommendation of test code (The Specification Compilation Group of the Ministry of Water Resources of the People's Republic of China 2001), the test pit is then filled with water to keep samples soaked for 48 hours (Fig. 3). Then, the direct shear tests are further performed using these saturated rock mass samples.

3.3 Test results

3.3.1 Typical test curves

Fig. 4 plots the shear stress *versus* displacement curves

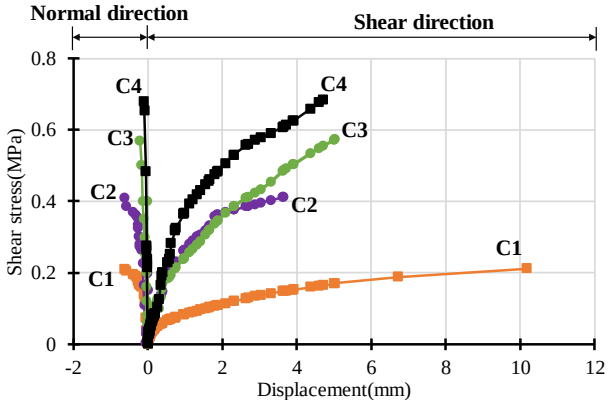

(a) Natural state

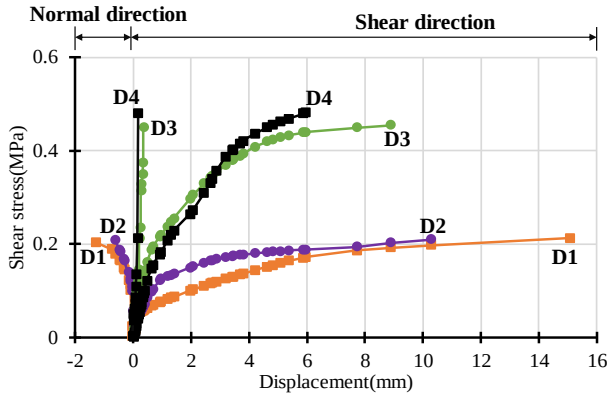

(b) Saturated state

Fig. 5 Shear stress *versus* displacement curves with shea loading direction parallel to bedding plane strike

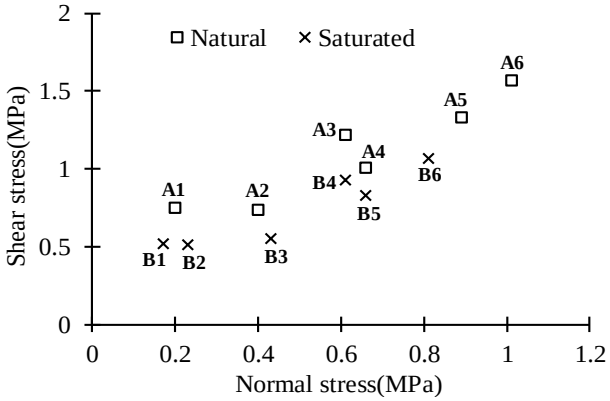

(a) Shear direction perpendicular to the strike of bedding planes

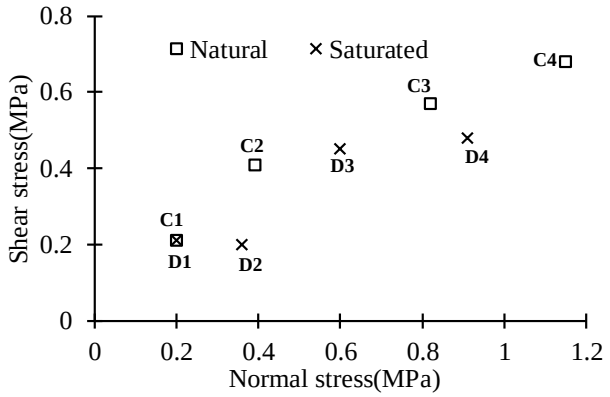

(b) Shear direction parallel to the strike of bedding planes

Fig. 6 Shear stress *versus* normal stress of the direction shear tests

for the thin-bedded rock masses with shear loading direction perpendicular to the strike of bedding plane. The negative values of X-axis refer to normal displacements of failure plane while the positive values refer to shear displacements. The normal stress increases gradually from A1/B1 to A6/B6, namely from 0.2 MPa to 1.0 MPa. It is observed that the displacements along shear direction is considerably larger than the values along normal direction. The displayed curves also indicate that the peak shear stress is generally in positive correlation with normal stress. For samples under natural state, the measured maximum normal and shear displacements of failure plane are 4.96 mm and 16.62 mm, respectively. For samples under saturated state, the measured maximum normal and shear displacements of failure plane are 5.23 mm and 17.42 mm, respectively. The occurrence of normal displacements of failure plane manifest the shear dilatancy characteristics of thin-bedded rock masses. The peak shear displacements under natural and saturated states are both roughly 3 times the peak shear displacements. The maximum shear and normal displacements under saturated state are larger than the values under natural state, indicating a certain extent of water softening effect on rock mass.

Fig. 5 plots the shear stress *versus* displacement curves for thin-bedded rock masses with shear loading direction parallel to the strike of bedding plane. The normal stress increases gradually from C1/D1 to C4/D4, namely from 0.2MPa to 1.2MPa. The variation laws of the obtained curves under increasing normal stress are consistent with those obtained from samples with shear loading direction perpendicular to the strike of bedding plane. For samples under natural state, the measured maximum normal and shear displacements of failure plane are 0.64 mm and 10.12 mm, respectively. For samples under saturated state, the measured maximum normal and shear displacements of failure plane are 1.30 mm and 15.05 mm, respectively. Although normal displacements still occur, their magnitude is significantly smaller, namely about 15%~20% of the normal displacement magnitudes obtained under the loading direction perpendicular to the strike of bedding plane. This remarkable difference show that the shear dilatancy effect of thin-bedded rock masses are much more weaker along the bedding plane direction. The peak shear displacements of natural state are all smaller than the values of saturated state. It can be understood that the water plays the role of layer lubricant for bedding plane.

3.3.2 Peak shear stress

Fig. 6 plots the results of peak shear stress *versus* normal stress based on the direct shear tests. It is summarized that under normal stress ranging from 0.2 MPa to 1.0 MPa, the obtained peak shear strength values are 0.75 MPa ~ 1.57MPa for natural state samples and 0.52 MPa ~ 1.07 MPa for saturated state samples. Also, it is shown that under normal stress from 0.2 MPa to 1.2 MPa, the obtained

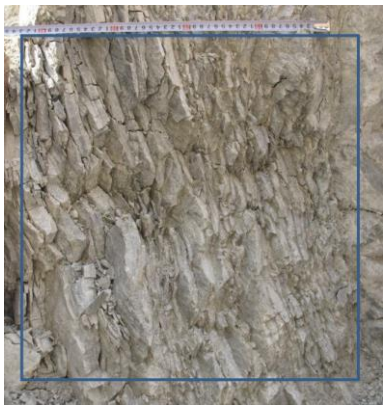

(a) Natural sample with normal stress of 0.61MPa

(b) Saturated sample with normal stress of 0.23MPa

Fig. 7 Failure planes of direct shear tests with shear loading direction perpendicular to the bedding plane strike (the rectangles refer to the location shear area)

peak shear strength values are 0.21 MPa ~ 0.68 MPa for natural state samples and 0.21 MPa ~ 0.48 MPa for saturated state samples. Following findings can be noted by observing obtained strength data.

- The peak shear stress of rock mass samples under natural state is higher than the peak shear stress under saturated state.
- The peak shear stress of rock mass samples perpendicular to the strike of bedding planes is higher than the peak shear stress parallel to the strike.
- The relationship between peak shear stress and corresponding normal stress shows an approximate linear relationship.

3.3.3 Failure planes of different loading directions

Fig. 7 plots typical failure planes of samples with shear loading direction perpendicular to the bedding plane strike. The failure type of samples under both natural state and saturated state is the shear rupture of host rocks. That is, the laminar host rock ruptures subjected to shear loading perpendicular to the strike of bedding planes. This shows that for such thin-bedded rock mass, its shear strength perpendicular to the bedding plane strike direction is governed by the shear strength of the laminar host rocks.

Fig. 8 plots typical failure planes of samples with shear loading direction parallel to the strike of bedding planes. The infillings of the bedding plane is phyllitic films. They become wet after the rock masses are soaked in water for 48h. The layer substances contains no mud and become powdery after hand twist. The failure plane images indicate that the failure type of these samples under both natural

(a) Saturated sample with normal stress of 0.36 MPa

(b) Saturated sample with normal stress of 0.60 MPa

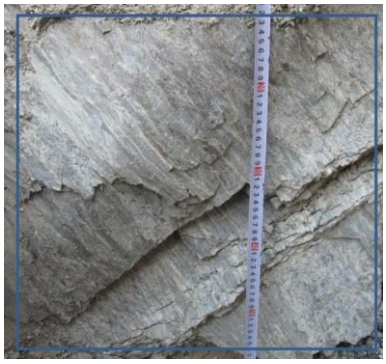

(c) Saturated sample with normal stress of 0.91 MPa

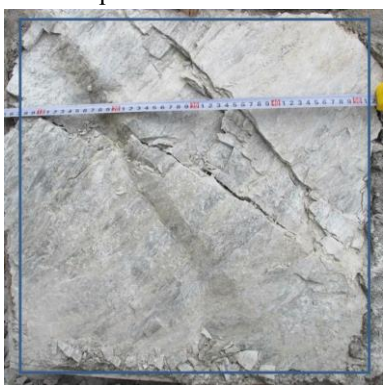

(d) Natural sample with normal stress of 1.15 MPa

Fig. 8 Failure planes of direct shear tests with shear loading direction parallel to the bedding plane strike

Table 1 Variation laws of Mohr-Coulomb shear strength parameters for thin layer rock masses under natural and saturated conditions

	Natural state			Saturated state			Variation	
	c /MPa	φ /°	tanφ	c /MPa	φ /°	tanφ	c	tanφ
⊥	0.45	45.8	1.03	0.30	42.0	0.90	-33%	-13%
∥	0.17	24.7	0.46	0.11	23.7	0.44	-35%	-4%

* ⊥ means the shear direction is perpendicular to bedding plane and ∥ means the shear direction is parallel to bedding plane.

state and saturated state is primarily the slip of bedding planes. That is, the bedding plane is dislocated subjected to shear loading parallel to the strike of bedding planes. Further, a variation in the failure characteristic of shear planes is observed with the increase of applied fixed normal stress. Because the rupture of laminar host rock is also present in a small proportion on the failure plane. A possible explanation to this phenomenon could be the role of friction on bedding planes. During the direct shear test, the increase of applied normal stress leads to the increase of friction acting on the interlayers and causes force difference among the interlayers of laminar host rocks. When the force difference, also called as relative friction, between the upper side and the lower side of a laminar rock exceeds the its tensile capacity, tensile rupture will occur.

In general, for direct shear test with its shear loading direction parallel to the strike of bedding planes, although tensile rupture of laminar rock occurs when the applied normal stress increases to a certain extent, the proportion of such tensile rupture on the failure plane is very small. Therefore, the shear strength of thin-bedded rock mass parallel to the strike of bedding planes is mainly governed by the shear strength of the bedding planes.

3.3.4 Characterization of mechanical parameters

The shear stress *versus* normal stress data in Fig. 6 suggest an approximate linear relationship, which is suitable to employ the Mohr-Coulomb criterion to characterize the quantitative mechanical properties. The test results in Fig. 6 are fitted using the least squares method. The shear strength lines under natural state and saturated state of the two groups are obtained. For shear direction perpendicular to the strike of bedding planes, the relations corresponding to natural state and saturated state are (1) and (2), respectively.

$$\tau = 1.03\sigma + 0.45 \quad (1)$$

$$\tau = 0.90\sigma + 0.30 \quad (2)$$

For shear direction parallel to the strike of bedding planes, the relations corresponding to natural state and saturated state are (3) and (4), respectively.

$$\tau = 0.46\sigma + 0.17 \quad (3)$$

$$\tau = 0.44\sigma + 0.11 \quad (4)$$

Thus, the anisotropic characteristics of thin-bedded rock mass and their variation under different water content can be quantified using the cohesion and internal friction angle indexes as shown in Table 1. It is indicated that for the two orthogonal directions, the cohesion and the internal friction coefficient are both reduced due to water immersion effect. But the cohesion value shows a greater decreasing extent.

The above work completes a quantitative evaluation of shear strength characteristics of thin-bedded rock masses under both natural and saturated conditions. The results provide a solid basis for evaluating the effect of mechanical property variation of the slope rock masses at Wudongde hydropower plant after reservoir impoundment.

4. Numerical investigation of the influence of rock mass degradation due to reservoir impoundment

4.1 Initial calculation conditions

The Nos. 3, 4, and 5 diversion tunnels plotted in Figure 9 are placed on the right bank of Wudongde hydropower plant. Nos. 3 and 4 diversion tunnels are 19.9 m×27.2 m (width×height), and their sidewalls are 21.2 m in height. No. 5 diversion tunnel is smaller with a dimension of 14.8 m×18.6 m (width×height) and the sidewalls are 14.1 m.

Numerical analysis was firstly carried out to analyze the rock mass stability of diversion tunnels during construction period. Fig. 9 plots the calculation mesh. Its dimension are 365 m×600 m×716 m and it comprises 329,483 nodes and 322,800 elements. The commercial software FLAC^{3D} is

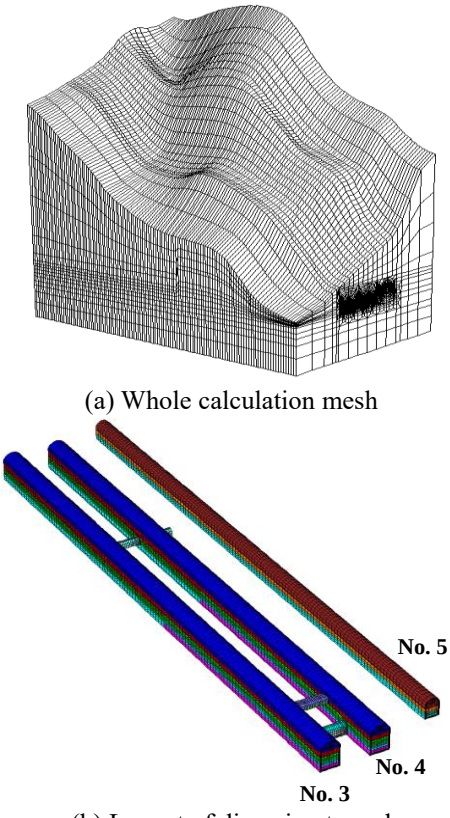

(a) Whole calculation mesh

(b) Layout of diversion tunnel

Fig. 9 Calculation mesh of the right bank diversion tunnels

Table 2 Mechanical parameters used in construction period

Mechanical parameters	E /GPa	Rock mass		Bedding plane	
		c/MPa	tanφ	c/MPa	tanφ
Outside EDZ	4.0	0.55	0.75	0.10	0.60
Within EDZ	0.6			0.07	0.55

Table 3 Variation of mechanical parameters subjected to reservoir impoundment

Mechanical parameters	Rock mass		Bedding plane	
	c/MPa	tanφ	c/MPa	tanφ
Outside EDZ	0.37	0.66	0.07	0.58
Within EDZ	0.37	0.66	0.05	0.53

adopted and the ubiquitous-joint plasticity model is used to model the thin-bedded stratified rock mass.

As revealed by field monitoring and observations, the measured surrounding rock mass deformation (over 110 mm) and the range of excavation damaged zone (EDZ, about 6~8 m) are significantly larger than other tunnels of similar excavation size. Despite this, the evaluation conclusions during construction period (Ding *et al.* 2017), which has been confirmed by field monitoring data, show that the surrounding rock mass stability can be achieved by using additional reinforcement measures. The adopted rock mass mechanical parameters are summarized in Table 2. The mechanical parameters for rock masses outside EDZ are determined based on field tests and recommended by geological engineers, and the values for rock masses within the range of EDZ are determined by regression method using field monitored deformation data. As the degradation of bedding plane within the extent of EDZ is much more significant than that of rock mass, only the variation of strength mechanical parameters of bedding plane is considered.

The above rock mass mechanical parameters and calculation results describe the diversion tunnel stability conditions under excavation and rock support effect. They act as the initial calculation conditions for subsequent evaluation of tunnel stability subjected to the reservoir impoundment during operation period.

4.2 Consideration of degradation of mechanical properties of rock masses after impoundment

It should be noted that, although the lithological condition and rock mass structure characteristics of the field test site are consistent with those of the diversion tunnels, there are still certain differences in strength parameters. The main reason to this issue is the rocks of the field test site undertake different weathering and excavation unloading effects compared to the surrounding rock mass of diversion tunnels.

Despite this, the field test provides an insight into the variation laws of mechanical properties for the thin-bedded rock mass under natural state and saturated state. Therefore, numerical evaluation mainly adopts the variation data of strength parameters listed in Table 1, by combining the parameters used in construction period listed in Table 2, to consider the degradation effect of rock masses in operation period.

In detail, the variation laws of shear strength parameters perpendicular to the bedding planes in Table 1 are used to reduce the mechanical parameters of rock masses. That is, the cohesion and internal friction coefficient of rock masses are reduced by 33% and 12%, respectively. The variation laws of shear strength parameters parallel to the bedding planes in Table 1 are used to reduce the mechanical parameters of rock mass bedding planes. That is, the cohesion and internal friction coefficient of the rock mass bedding planes are reduced by 35% and 4%, respectively. The shear strength parameters listed in Table 3 are adopted to consider the influences of reservoir impoundment, which may turn the surrounding rock mass of diversion tunnels from natural state to water-saturated state.

Moreover, the variation of water level due to reservoir impoundment is considered. The water level during diversion tunnel construction period is about 810m and it will rise to 920.88m during operation period, corresponding to a flood frequency with recurrence interval of 20 years. The numerical simulation considers the effect of water level by subtracting pore pressure from total stress. Therefore, the elements beneath the water level use the effective stress in numerical calculation.

4.3 Analysis of surrounding rock mass stability

No.5 diversion tunnel is smaller in size and more distant from Nos 3 and 4 tunnels. The rock mass around No. 5 tunnel has a different lithology with the studied rock mass. Therefore, the analysis below mainly covers the results of Nos 3 and 4 tunnels.

The stability conditions are analyzed in terms of rock deformation and stress in support measures. Fig. 10 plots the contours of horizontal incremental deformation of surrounding rock masses. It is discovered that the incremental horizontal deformation is within 18mm and the maximum value occurs at the middle of the right sidewall of No. 4 diversion tunnel. Compare to the deformation induced by excavation, the incremental deformation is much smaller. A check of the stresses in anchor bolts and cables indicates that the incremental stresses are small. For anchor bolts, their average stresses increase 19MPa after impoundment. For anchor cables, their average forces

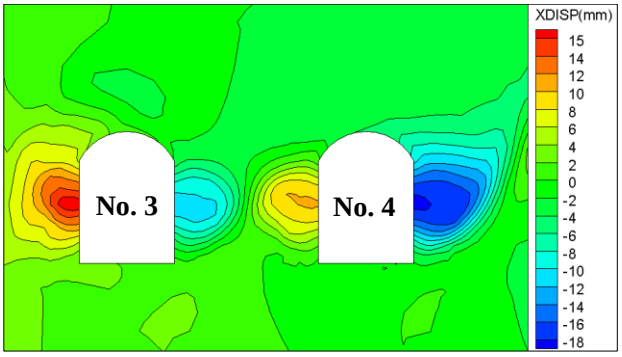

Fig. 10 Contours of horizontal incremental deformation

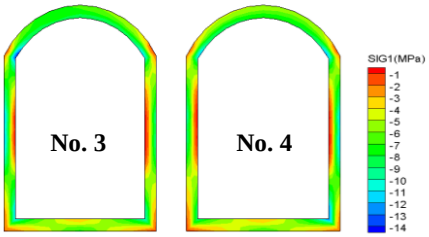

(a) Contours of the first principal stress

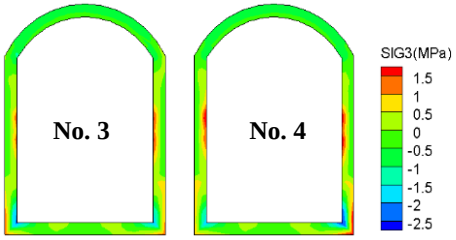

(b) Contours of the third principal stress

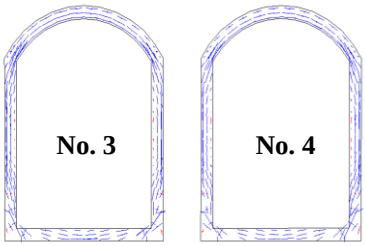

(c) Principal vectors, where lines in blue are in compressive state and lines in red are tensile state

Fig. 11 Principal stresses in lining structure

increase 66 kN. In general, neither bolt stresses nor cable forces reach their yield value.

4.4 Analysis of stresses in lining structures

The lining structures use C40-class concrete at the floor and C30-class concrete at other parts of the diversion tunnels. Fig, 11 plots the results. It is found that the first principal stresses range from -14.2 MPa~ -0.5 MPa and the third principal stresses range from -2.67 MPa~1.55 MPa. The principal stress vectors indicate that the inner edge areas at the middle of the sidewall are in tensile state. By proper steel reinforcement, the structural stability of lining structures can be guaranteed.

5. Conclusions

Focusing on the anisotropic characteristics of a natural thin-bedded rock mass and its strength variation subjected to water immersion, this paper provides a case-based study using field test method rather than traditional core drilling method to investigate the mechanical properties of the mentioned rock mass. The highlight of field test is the use of large size samples with a shear dimension of 0.5m*0.5m, representing a more realistic in-situ situation than small size specimen. Following findings can be noted.

• The concerned issue involved in the studied case will be encountered more frequently in the future, because a large number of hydropower plants will be completed in China in the next one or two decades. As reservoir impoundment is a necessary procedure of power generation, the rock masses of nearby slope banks and the tunnels excavated in this region all face water immersion effect, which degrades the rock mass property and causes potential threat to rock projects.

• The focused thin-bedded rock masses have the nature of high anisotropy. The field test serves as a necessary tool to investigate the shear strength characteristics both parallel and perpendicular to the strike of bedding planes. The test reveals that the shear strengths of thin-bedded rock masses are reduced due to water immersion effect, and the cohesion values and friction values are decreased in different extents. The variation laws of shear strength from natural state to saturated state derived from field tests are consistent with the conclusions reported by other literatures, in which laboratory experiments are common ways and the rock samples often contains limited numbers of joint and fracture planes. Despite this, the field test results provide a fundamental quantitative basis for evaluating the rock mass stability of diversion tunnels subjected to the influences caused by reservoir impoundment.

• The numerical simulation results show that after impoundment, the incremental deformation of surrounding rocks of the tunnels and the incremental stresses in anchor bolts and cables are small. The structural stability of the lining structures can be guaranteed by proper steel reinforcement, based on the calculated stress results.

Finally, the work of this paper presents an “experimental plus numerical” approach for solving practical engineering issues encountered in a major hydropower plant that is currently under construction in China. The findings of field test on thin-bedded rock masses and the numerical evaluation procedures on surrounding rock mass stability of tunnels after impoundment are hoped to provide references for rock projects with similar concerns.

Acknowledgments

The work was supported by the National Natural Science Foundation of China (Nos. 51539002 and 51779018) and the Basic Research Fund for Central Research Institutes of Public Causes (Nos. CKSF2019434/YT and CKSF2019169/YT).

References

Alemdag, S., Gurocak, Z., Cevik, A., Cabalar, A.F. and Gokceoglu, C. (2016), “Modeling deformation modulus of a stratified sedimentary rock mass using neural network, fuzzy inference and genetic programming”, *Eng. Geol.*, **203**, 70-82. https://doi.org/10.1016/j.enggeo.2015.12.002.

Aydan, Ö., Ulusay, R. and Tokashiki, N (2014), “A new rock mass quality rating system: rock mass quality rating (RMQR) and its application to the estimation of geomechanical characteristics of rock masses”, *Rock Mech. Rock Eng.*, **47**(4), 1255-1276. https://doi.org/10.1007/s00603-013-0462-z.

Ding, X., Weng, Y., Zhang, Y., Xu, T., Wang, T., Rao, Z. and Qi, Z. (2017), “Stability of large parallel tunnels excavated in weak

rocks: A case study", *Rock Mech. Rock Eng.*, **50**(9), 2443-2464. https://doi.org/10.1007/s00603-017-1247-6.

Fortsakis, P., Nikas, K., Marinos, V. and Marinos, P. (2012), "Anisotropic behaviour of stratified rock masses in tunnelling", *Eng. Geol.*, **141**, 74-83. https://doi.org/10.1016/j.enggeo.2012.05.001.

Gokceoglu, C. and Aksoy, H. (2000), "New approaches to the characterization of clay-bearing, densely jointed and weak rock masses", *Eng. Geol.*, **58**(1), 1-23. https://doi.org/10.1016/S0013-7952(00)00032-6.

Gu, H., Tao, M., Wang, J., Jiang, H., Li, Q. and Wang, W. (2018), "Influence of water content on dynamic mechanical properties of coal", *Geomech. Eng.*, **16**(1), 85-95. https://doi.org/10.12989/gae.2018.16.1.085.

Hoek, E., Marinos, P.G. and Marinos, V.P. (2005), "Characterisation and engineering properties of tectonically undisturbed but lithologically varied sedimentary rock masses", *Int. J. Rock Mech. Min. Sci.*, **42**(2), 277-285. https://doi.org/10.1016/j.ijrmms.2004.09.015.

https://doi.org/10.1016/j.enggeo.2018.12.023.

Ishida, T., Kanagawa, T. and Kanaori, Y. (2010), "Source distribution of acoustic emissions during an in-situ direct shear test: Implications for an analog model of seismogenic faulting in an inhomogeneous rock mass", *Eng. Geol.*, **110**(3-4), 66-76. https://doi.org/10.1016/j.enggeo.2009.11.003.

Kim, E. and Changani, H. (2016), "Effect of water saturation and loading rate on the mechanical properties of Red and Buff Sandstones", *Int. J. Rock Mech. Min. Sci.*, (88), 23-28. http://dx.doi.org/10.1016%2Fj.ijrmms.2016.07.005.

Kundu, J., Mahanta, B., Sarkar, K. and Singh, T.N. (2018), "The effect of lineation on anisotropy in dry and saturated Himalayan Schistose Rock under Brazilian test conditions", *Rock Mech. Rock Eng.*, **51**(1), 5-21. https://doi.org/10.1007/s00603-017-1300-1305.

Liu, K. and Sheng, J.J. (2019), "Experimental study of the effect of stress anisotropy on fracture propagation in Eagle Ford shale under water imbibition", *Eng. Geol.*, **249**, 13-22.

Liu, X., Liu, Q., Liu, B., Zhu, Y. and Zhang, P. (2019), "Failure behavior for rocklike material with cross crack under biaxial compression", *J. Mater. Civ. Eng.*, **31**(2), 06018025. https://doi.org/10.1061/(ASCE)MT.1943-5533.0002540.

Marinos, V. (2019), "A revised, geotechnical classification GSI system for tectonically disturbed heterogeneous rock masses, such as flysch", *Bull. Eng. Geol. Environ.*, **78**(2), 899-912. https://doi.org/10.1007/s10064-017-1151-z.

Palmström, A. and Singh, R. (2001), "The deformation modulus of rock masses—comparisons between in situ tests and indirect estimates", *Tunn. Undergr. Sp. Technol.*, **16**(2), 115-131. https://doi.org/10.1016/S0886-7798(01)00038-4.

Pellet, F.L., Keshavarz, M. and Boulon, M. (2013), "Influence of humidity conditions on shear strength of clay rock discontinuities", *Eng. Geol.*, **157**, 33-38. https://doi.org/10.1016/j.enggeo.2013.02.002.

Roy, D.G., Singh, T.N., Kodikara, J. and Das, R. (2017), "Effect of water saturation on the fracture and mechanical properties of sedimentary rocks", *Rock Mech. Rock Eng.*, **50**(10), 2585-2600. https://doi.org/10.1007/s00603-017-1253-8.

Tang, S.B., Yu, C.Y., Heap, M.J., Chen, P.Z. and Ren, Y.G. (2018), "The influence of water saturation on the short-and long-term mechanical behavior of red sandstone", *Rock Mech. Rock Eng.*, **51**(9), 2669-2687. https://doi.org/10.1007/s00603-018-1492-3.

The Specification Compilation Group of the Ministry of Water Resources of the People's Republic of China (2001), *Specification for Rock Tests in Water Conservancy and Hydroelectric Engineering(SL264-2001)*, China Water and Power Press, Beijing, China.

Umrao, R.K., Sharma, L.K., Singh, R. and Singh, T.N. (2018), "Determination of strength and modulus of elasticity of heterogenous sedimentary rocks: An ANFIS predictive technique", *Measurement*, **126**, 194-201. https://doi.org/10.1016/j.measurement.2018.05.064.

Xing, H., Liu, L. and Luo, Y. (2019), "Water-induced changes in mechanical parameters of soil-rock mixture and their effect on talus slope stability", *Geomech. Eng.*, **18**(4), 353-362. https://doi.org/10.12989/gae.2019.18.4.353.

Zhang, F., Cui, Y., Zeng, L., Robinet, J.C., Conil, N. and Talandier, J. (2018), "Effect of degree of saturation on the unconfined compressive strength of natural stiff clays with consideration of air entry value", *Eng. Geol.*, **237**, 140-148. https://doi.org/10.1016/j.enggeo.2018.02.013.

Zhao, Y., Liu, S., Jiang, Y., Wang, K. and Huang, Y. (2016), "Dynamic tensile strength of coal under dry and saturated conditions", *Rock Mech. Rock Eng.*, **49**(5), 1709-1720. https://doi.org/10.1007/s00603-015-0849-0.

Zhao, Z., Yang, J., Zhou, D. and Chen, Y. (2017), "Experimental investigation on the wetting-induced weakening of sandstone joints", *Eng. Geol.*, **225**, 61-67. https://doi.org/10.1016/j.enggeo.2017.04.008.

Zhou, Z., Cai, X., Cao, W., Li, X. and Xiong, C. (2016), "Influence of water content on mechanical properties of rock in both saturation and drying processes", *Rock Mech. Rock Eng.*, **49**(8), 3009-3025. https://doi.org/10.1007/s00603-016-0987-z.

CC